LOCKHEED MARTIN ENERGY RESEARCH LIBRARIES
3 4456 0514899 8

CENTRAL RESEARCH LIBRARY

ORNL-TM-3944

cy. 84

NEUTRON CROSS-SECTION SENSITIVITY ANALYSIS: A GENERAL APPROACH ILLUSTRATED FOR A Na-Fe SYSTEM

D. E. Bartine
E. Oblow
F. R. Mynatt

OAK RIDGE NATIONAL LABORATORY
CENTRAL RESEARCH LIBRARY
DOCUMENT COLLECTION
LIBRARY LOAN COPY
DO NOT TRANSFER TO ANOTHER PERSON
If you wish someone else to see this document, send in name with document and the library will arrange a loan.
UCN-7969
(3 3-67)

OAK RIDGE NATIONAL LABORATORY
OPERATED BY UNION CARBIDE CORPORATION • FOR THE U.S. ATOMIC ENERGY COMMISSION

This report was prepared as an account of work sponsored by the United States Government. Neither the United States nor the United States Atomic Energy Commission, nor any of their employees, nor any of their contractors, subcontractors, or their employees, makes any warranty, express or implied, or assumes any legal liability or responsibility for the accuracy, completeness or usefulness of any information, apparatus, product or process disclosed, or represents that its use would not infringe privately owned rights.

ORNL-TM-3944

Contract No. W-7405-eng-26

Mathematics Division

NEUTRON CROSS-SECTION SENSITIVITY ANALYSIS: A GENERAL APPROACH ILLUSTRATED FOR A Na-Fe SYSTEM

D. E. Bartine, E. Oblow,* and F. R. Mynatt*

NOTE:

This Work Funded by
DEFENSE NUCLEAR AGENCY PROGRAM
in the
NEUTRON PHYSICS DIVISION
Under Subtask PC104

DECEMBER 1972

*Neutron Physics Division.

NOTICE This document contains information of a preliminary nature and was prepared primarily for internal use at the Oak Ridge National Laboratory. It is subject to revision or correction and therefore does not represent a final report.

OAK RIDGE NATIONAL LABORATORY
Oak Ridge, Tennessee 37830
operated by
Union Carbide Corporation
for the
U.S. ATOMIC ENERGY COMMISSION

LOCKHEED MARTIN ENERGY RESEARCH LIBRARIES
3 4456 0514899 8

Abstract

A general approach to sensitivity studies is introduced using a quantitative definition of cross-section sensitivity. The definition offered is intended to be both practical and physically meaningful. Its advantages in comparison with other approaches are discussed and its use in analysis is illustrated for a sodium-iron transport problem. Results of the analysis include a discussion of the role of important total cross-section minima in deep penetration in sodium and iron and the importance of certain energy ranges and partial cross sections for the sodium-iron system. The predictive aspect of the approach is demonstrated in comparisons of rigorous and predicted results for small cross-section perturbations and in conclusions about the order of Legendre expansion of the scattering kernel.

I. INTRODUCTION

Sensitivity analysis, the procedure by which one determines how sensitive a calculated result is to microscopic cross-section data, is finding ever-increasing applicability in shielding research. This trend is a direct result of the successful application of transport methods to shield analysis and the demand they create for more accurate cross-section data. With growing acceptance of the accuracy of these techniques, sensitivity studies have begun to play a major role in the task of uncovering cross-section inadequacies through analysis of integral experiments and determining their impact on overall shield design.

In practice, sensitivity studies fall into two broad categories: (1) those characterized by calculations made with differing data sets,[1-4] and (2) methods based on the use of adjoint fluxes and perturbation theory.[5-7] Most work to date has been concentrated in the first area, but the methods employed in both of these groupings have strengths and weaknesses that govern their applicability in any specific instance. Assuming the positive aspects are well understood, two inherent limitations should be pointed out. In studies characterized by the use of differing data sets, there is a practical limit to the number of data sets or cross-section changes which can be analyzed. Additionally, computer arithmetic limits the size of changes which can be made while still retaining significance in computed results. The perturbation approach, as presently used, suffers from the constraints of first-order perturbation theory, which usually limits analysis to the effects of small cross-section changes. Also, there has been a tendency to leave the practical goal of the sensitivity study vaguely defined when using this method,

with the result that applications have chiefly been concerned with the effects of energy-dependent cross-section changes on the energy dependence of the scalar flux. In this instance, for practical applications, an enormous amount of information is available for analysis and it can be a question of "not seeing the forest for the trees."

Our approach to the problem of sensitivity analysis has been to recognize the inherent advantages of the perturbation model (e.g., for studying large amounts of data), and simply modify the approach so as to make it more practically oriented and to increase the physical relevance of the results produced. In this light, the method has been restricted to an analysis of the sensitivity of a flux-integrated quantity (such as dose, fluence, etc.) to basic cross-section data. The results are then of practical interest to shield designers and, in addition, make sensitivity a more problem-dependent concept. From the large number of choices of functional form for the sensitivity profiles, trial and error leads to a form which seems to convey maximum physical insight. The following definition of the "sensitivity profile," $P_\Sigma(E)$, is thus offered:

$$P_\Sigma(E) \equiv \frac{\int_{\bar{\Omega}} \int_{\bar{r}} N^*(\bar{r},E,\bar{\Omega}) T_\Sigma N(\bar{r},E,\bar{\Omega}) d\bar{r} d\bar{\Omega}}{R} \tag{1}$$

where

$$R = \int_{\bar{r},E,\bar{\Omega}} \Sigma_R(\bar{r},E,\bar{\Omega}) N(\bar{r},E,\bar{\Omega}) d\bar{r} dE d\bar{\Omega} \tag{2}$$

is the flux-integrated response for response function Σ_R, N^* is the adjoint flux, N is the forward flux, and T_Σ is a reaction operator for the partial cross section whose sensitivity profile is being calculated. For cases where T_Σ includes transfer cross sections, $N^*T_\Sigma N$ should be understood to imply an integration over final energy of the product of the transfer rate from E to final energy E_f and the importance at E_f [i.e., $\int_{E_f} N^*(E_f)\ T_{\Sigma(E,E_f)}\ N(E)\ dE_f$].

The physical meaning of the function $P_\Sigma(E)$ is almost evident from the way it is defined. $T_\Sigma N$ represents a reaction rate for partial cross-section Σ at energy E, and $N^*T_\Sigma N$ is then an importance weighting of the reaction rate (importance being represented by the adjoint flux N^*) as it relates to the response represented by R. Thus, the physical content of the sensitivity profile, as an importance-weighted energy-dependent reaction rate, can serve as a powerful tool for analyzing any calculation for the importance of each energy-dependent reaction process as it affects the final results.

In terms of the sensitivity of the response R to cross-section changes, the sensitivity profile rigorously represents the local logarithmic rate of change of R with respect to changes in reaction operator T_Σ at energy E, that is,

$$P_\Sigma(E) = \frac{\partial(\ell nR)}{\partial(\ell nT_\Sigma)} = \frac{\partial R/R}{\partial\Sigma/\Sigma} = \frac{\int_{\bar{r}}\int_{\bar{\Omega}} N^*T_\Sigma N d\bar{r}d\bar{\Omega}}{R} . \tag{3}$$

Here, use is made of the fact that T_Σ is simply an operator notation for the reaction cross section Σ which in general includes double differential data as well as partial cross sections. It is this derivative feature of the definition that allows one, within the framework of

perturbation theory, to predict changes in the response function resulting from finite changes in the cross-section data. Thus, one integrates the profile multiplied by an energy-dependent cross-section change to get the change in the response as:

$$\frac{\delta R}{R} \cong \int_{E} \frac{\delta\Sigma}{\Sigma} P(E)dE = \frac{\int_{\bar{E}} \int_{\bar{r}} \int_{\bar{\Omega}} N^* \delta T_{\Sigma} N d\bar{r} d\bar{\Omega} dE}{R} . \tag{4}$$

In this context, the use of N^*, the unperturbed adjoint, implies that linear perturbation theory is adequate for predicting R. Equation 4, however, is more general in that it is also possible to obtain rigorous results (which include non-linear effects) if the perturbed adjoint N_p^* is used in the original definition, in place of N^*.

Finally, the definition offered in Equation 3 is clearly quite practical in that large amounts of cross-section data can be processed for a sensitivity analysis with the results of only one forward and one adjoint calculation. Yet each cross-section process will have its own profile and each profile is unique for the particular problem being studied. Sensitivity is thus unambiguously defined in a problem-dependent manner, taking into account the effects of the specific source, detector, and material configuration used, as well as cross-section considerations.

II. ANALYSIS OF A Na-Fe SYSTEM

To illustrate both the analytic aspect of using a physically meaningful definition of sensitivity and the predictive aspect associated with perturbation theory, a particularly interesting problem of transport in a sodium-iron shield was investigated. The problem consists of a

neutron spectrum incident on a slab made up of 15 ft of sodium followed by 3 ft of iron. The calculations were performed with the one-dimensional discrete ordinates transport code, ANISN,[8] and the objective was the determination of the neutron tissue dose, as defined by a Snyder-Neufeld[9] response function, at the exit face of the iron zone. Specifically, the source used was the neutron leakage spectrum from the FTR radial shield as calculated using DOT[10] (a source peaked in the 300 keV to thermal energy range). The forward and adjoint ANISN calculations required were made using the 50-group energy structure employed at ORNL for FFTF design support calculations. Table 1 gives the details of the energy group structure, source spectrum, and tissue dose response function utilized in this analysis. The sodium cross sections used were those given in ENDF/B-III as Mat. 1156, and the iron cross sections were ENDF/B-III, Mat. 1180, which was re-evaluated using the recent total cross-section measurements of J. A. Harvey[11] for minima below 400 keV. The sensitivity of this problem to a specific cross section, as defined by Equation 3, was determined for each cross section used in the transport calculation. In addition, sensitivity profiles were obtained for each of the partial reaction cross sections listed in the ENDF/B-III files for sodium and iron.

Figure 1 presents the sensitivity of the tissue dose to the total collision cross section in the sodium. Each bar of the histogram represents the summed sensitivities of all the cross sections for a particular group divided by the lethargy width of that group. The peaks generally correspond to minima in the total cross section, for example those minima at 0.3, 1.9, and 3.0 MeV. It is most interesting to note here that the

Table 1. Group Structure, Source Spectrum, and Detector Response Function for Na-Fe Problem

Group	Upper Energy (eV)	Tissue Dose Factor (mrem/hr/n/cm^2/sec)	Source (n/sec)	Group	Upper Energy (eV)	Tissue Dose Factor (mrem/hr/n/cm^2/sec)	Source (n/sec)
1	14.92(+6)	0.150	4.3(-8)	26	8.652(+4)	0.0245	6.72(-2)
2	12.214(+6)	0.150	1.9(-7)	27	5.2475(+4)	0.0194	4.3(-2)
3	10.000(+6)	0.150	6.7(-7)	28	4.087(+4)	0.0162	3.5(-2)
4	8.187(+6)	0.149	1.8(-6)	29	3.183(+4)	0.0126	3.6(-2)
5	6.7032(+6)	0.143	3.9(-6)	30	2.479(+4)	0.0095	4.5(-2)
6	5.4881(+6)	0.136	7.2(-6)	31	1.930(+4)	0.0080	3.2(-2)
7	4.4933(+6)	0.132	1.2(-5)	32	1.503(+4)	0.0064	7.97(-2)
8	3.6788(+6)	0.129	2.5(-5)	33	7.102(+3)	0.0048	3.05(-2)
9	3.0119(+6)	0.126	3.52(-5)	34	4.307(+3)	0.0044	4.3(-3)
10	2.466(+6)	0.126 0.128	4.4(-5)	35	3.355(+3)	0.0045	8.1(-4)
11	2.019(+6)	0.128	8.1(-5)	36	2.613(+3)	0.0045	9.8(-3)
12	1.653(+6)	0.131	1.2(-4)	37	2.035(+3)	0.0046	2.6(-2)
13	1.353(+6)	0.134	1.6(-4)	38	1.585(+3)	0.0046	3.5(-2)
14	1.108(+6)	0.135	2.23(-4)	39	1.234(+3)	0.0047	3.3(-2)
15	9.072(+5)	0.122	3.2(-4)	40	9.611(+2)	0.0048	8.02(-2)
16	7.427(+5)	0.106	1.3(-3)	41	4.540(+2)	0.0049	5.91(-2)
17	6.081(+5)	0.091	3.8(-3)	42	2.145(+2)	0.0050	4.93(-2)
18	4.979(+5)	0.080	4.3(-3)	43	1.013(+2)	0.0050	4.23(-2)
19	4.076(+5)	0.073	9.0(-3)	44	4.785(+1)	0.0050	3.4(-2)
20	3.337(+5)	0.067	1.656(-2)	45	2.260(+1)	0.0050	2.8(-2)
21	2.732(+5)	0.060	1.7(-2)	46	1.068(+1)	0.0050	2.2(-2)
22	2.237(+5)	0.053	1.7(-2)	47	5.043(+0)	0.0050	1.5(-2)
23	1.832(+5)	0.046	2.24(-2)	48	2.382(+0)	0.0050	9.8(-3)
24	1.500(+5)	0.040	2.7(-2)	49	1.125(+0)	0.0050	6.09(-3)
25	1.228(+5)	0.031	5.6(-2)	50	0.414(+0)	0.00375	1.5(-3)
					Thermal ($\sim 1 \times 10^{-4}$)		

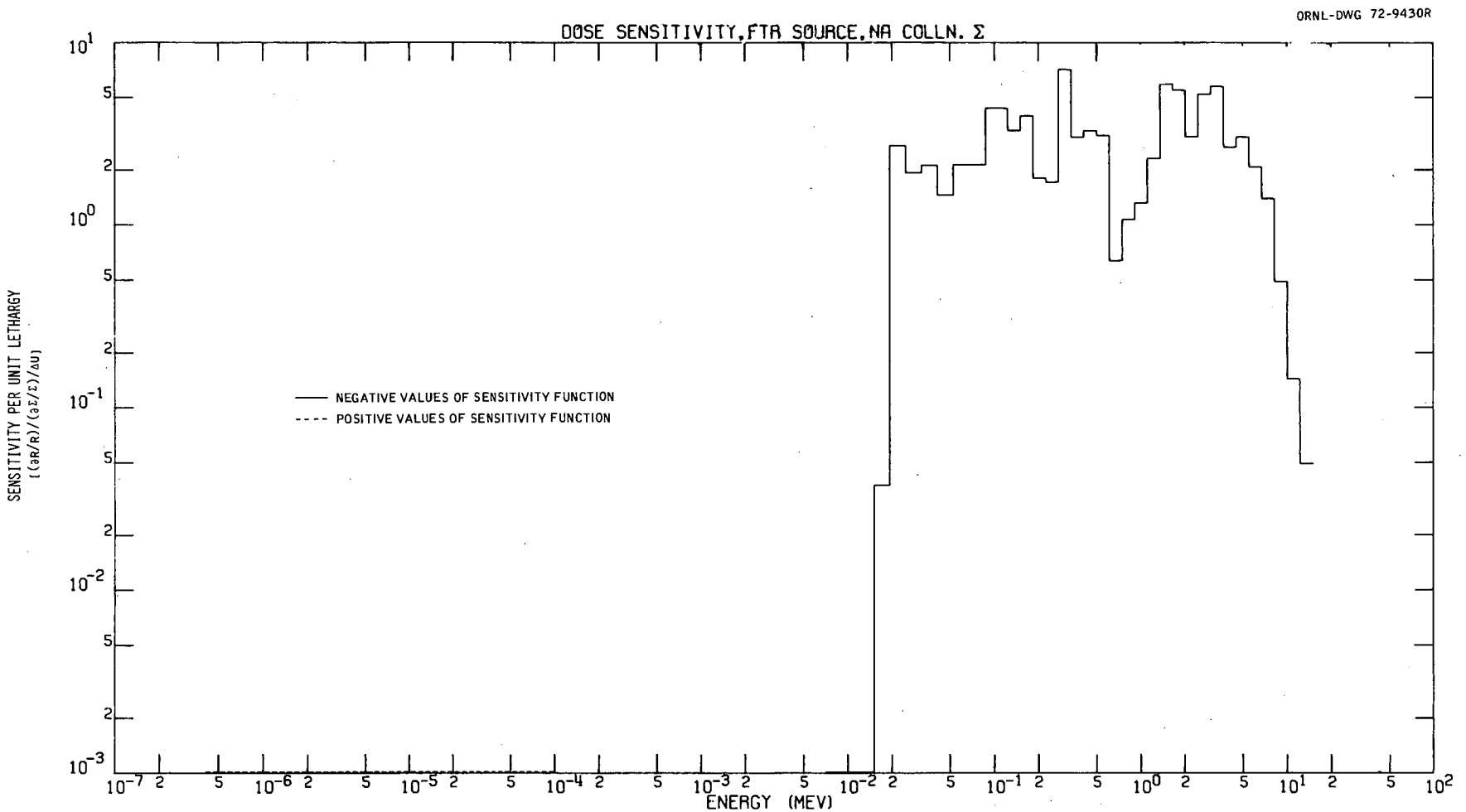

Fig. 1. Tissue Dose Sensitivity for Sodium Total Collision Cross Sections with FTR Source.

sensitivity above 1 MeV is extraordinarily high considering the small number of source neutrons in this energy range (see Table 1), and that the sensitivity drops off sharply below 24 keV. The lower cutoff is due to the fact that the deepest minimum in iron is the bin window at 24.5 keV, below which the iron greatly attenuates neutrons. The high energy importance is due largely to the moderating characteristics and thickness of the sodium slab (15 ft), which result in the high-energy source particles having a greater probability of entering the iron slab with energies above 24.5 keV. Additionally, as shown in Table 1, the dose response function decreases quite rapidly for lower energy neutrons.

This problem is therefore very sensitive to the high-energy sodium cross sections and to the total cross-section minima above 24.5 keV which serve as windows for the sodium transport. Analysis of the sensitivity to elastic and total inelastic cross sections for sodium, as shown in Fig. 2, indicates that the elastic cross section is predominant below 2 MeV, accounting for the peak at 1.9 MeV, while the inelastic cross section has increasing importance at higher energies, and accounts for the peak at 3 MeV.

Figure 3 gives the sensitivity profile for the total collision cross section in iron. The spectrum entering the iron slab is quite soft, due to the effects of slowing down in sodium and very few neutrons enter the iron with energies above 24.5 keV. The overall sensitivity of the problem to the iron cross sections therefore is much lower than the sensitivity to sodium cross sections. As could be expected, the iron sensitivity profile is dominated by the 24.5 keV minimum which is the widest and deepest window in the total cross section. Other prominent features correspond

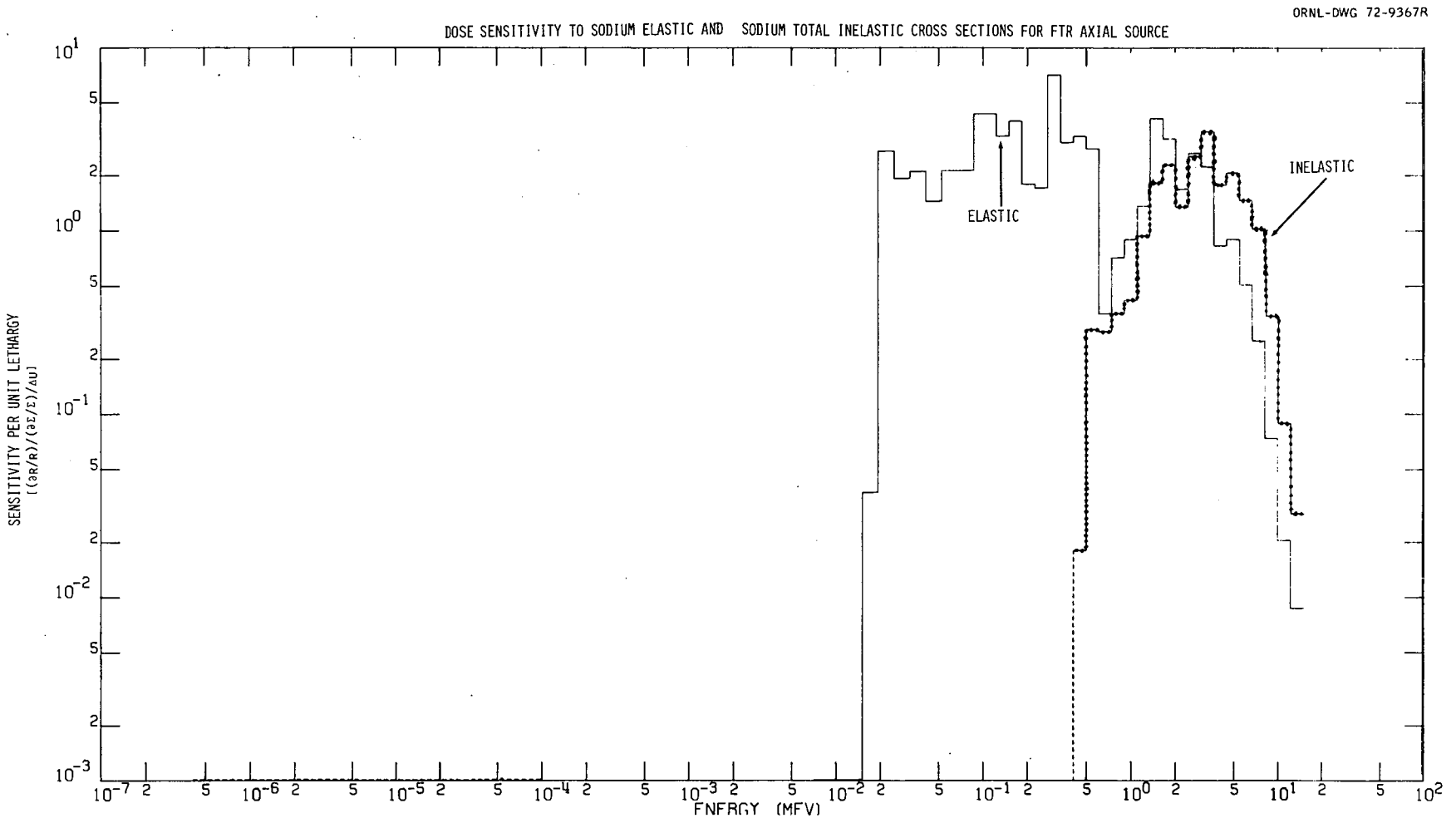

Fig. 2. Tissue Dose Sensitivity for Sodium Elastic and Total Inelastic Cross Sections with FTR Source.

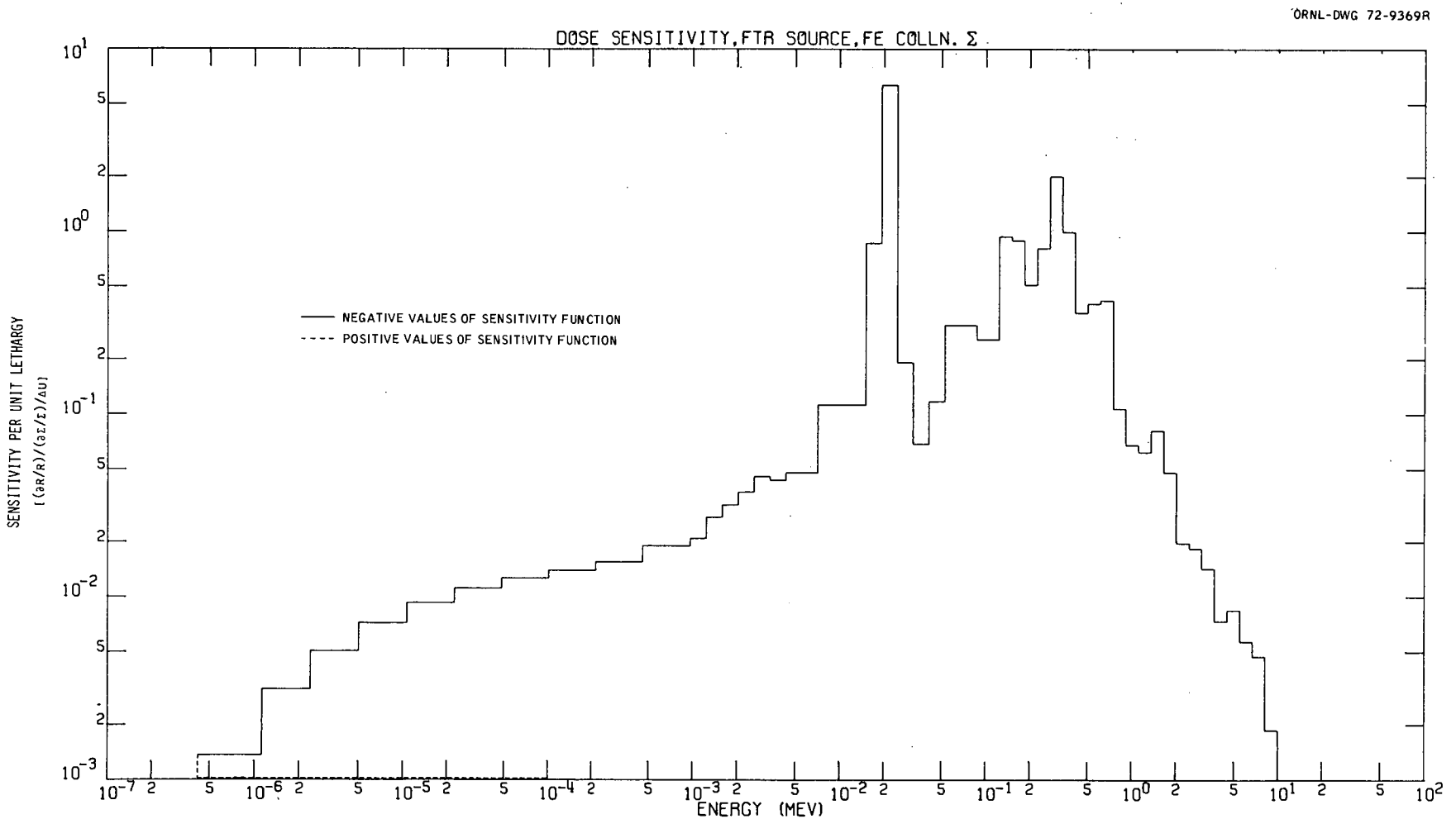

Fig. 3. Tissue Dose Sensitivity for Iron Total Collision Cross Sections with FTR Source.

to the minima at 170 and 300 keV. Sensitivity studies of the individual reaction cross sections for iron indicate that the elastic cross section is dominant for this problem, accounting for approximately 95% of the total sensitivity, as shown in Fig. 4. The two regions of positive sensitivity (dotted lines at $\sim$ 1 MeV and 1 keV) indicate that increasing the elastic cross sections in these groups results in an increase in the response function. At 1 MeV elastic scattering drops neutrons below the inelastic threshold, thereby increasing their probability of reaching the detector with higher energies. At 1 keV, however, elastic scattering prevents neutron absorption in the strong 1 keV capture resonance in this group. In general, positive effects as a result of increased elastic scattering occur in energy regions where a highly probable nonelastic event would have a strong negative effect on the response.

The sensitivity to the iron inelastic cross sections is shown in Fig. 5. It is noticably lower than the corresponding elastic profile mainly because of the extremely small number of neutrons which enter the iron above 1 MeV from the sodium region. Relatively speaking, however, it is clear that the important inelastic events are those just above the 846 keV threshold of the first excited state in iron. These events result in inelastically scattered neutrons which have energies in the vicinity of the prominent 24.5-keV minimum. This importance is further demonstrated by the second peak in Fig. 5 just below 2 MeV. This peak is the result of first-level inelastic events which feed the 1 MeV range. It is not the result of excitation of the second level which is at 2.05 MeV but rather the effect of multiple first-level events feeding the 24.5 MeV minimum.

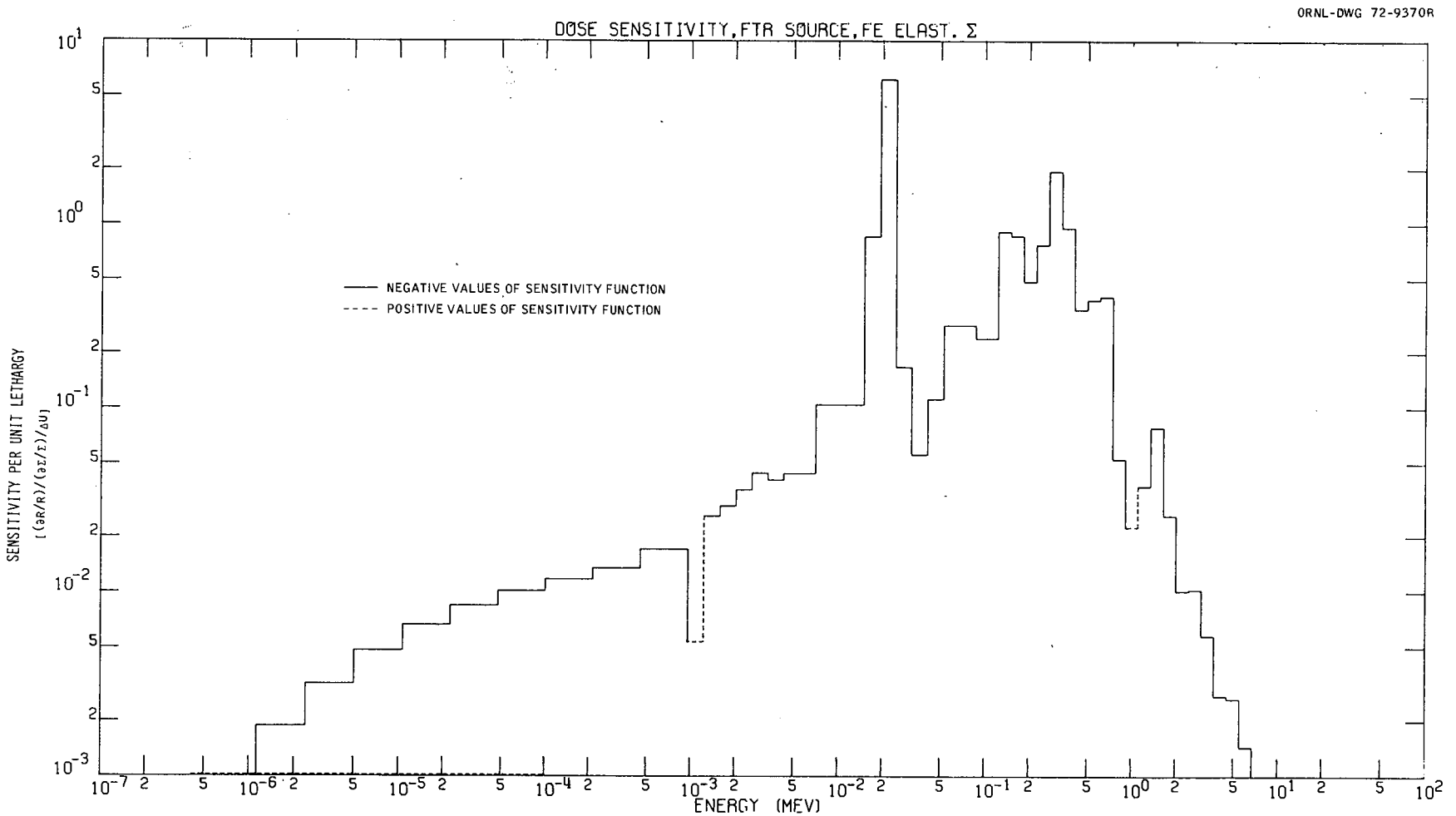

Fig. 4. Tissue Dose Sensitivity for Iron Elastic Cross Sections with FTR Source.

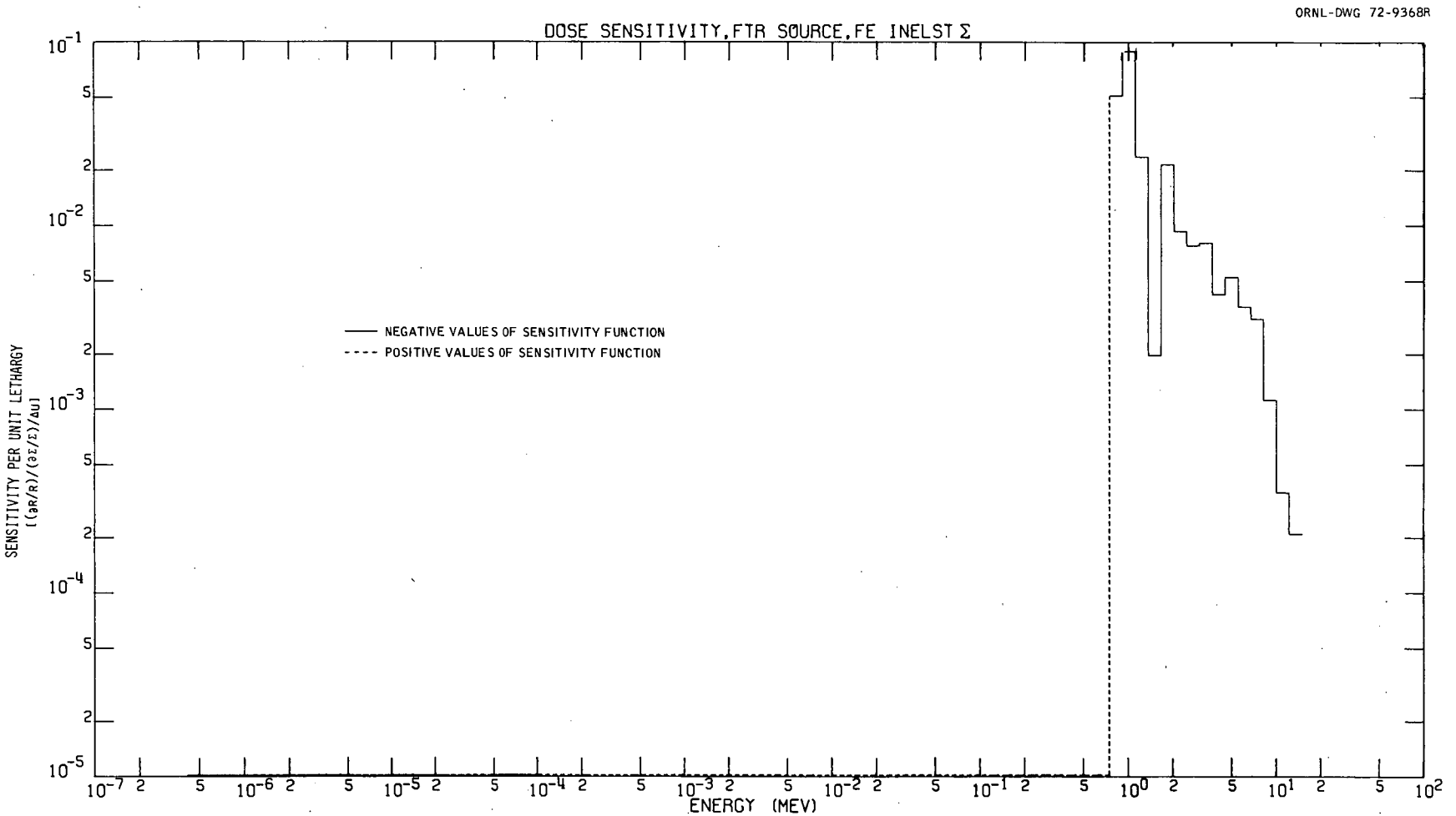

Fig. 5. Tissue Dose Sensitivity for Iron Total Inelastic Cross Sections with FTR Source.

A close inspection of the sensitivity profiles given here reveals the reduced importance or absence of peaks corresponding to certain important cross-section minima, such as those at 0.5 MeV in sodium or at 80 keV in iron. Examination of the point cross-section data, however, reveals that the group structure employed tended to mask these minima, and perhaps therefore incorrectly reduce their importance in the sensitivity profile. Future sensitivity studies will employ calculations using point cross sections or tailored group structures which adequately represent the cross-section detail.

The predictive aspect of this sensitivity technique was investigated using Equation 4 with the unperturbed adjoint flux. Table 2 presents some of the results of this study. The change in the tissue dose caused by increasing all sodium or all iron cross sections for all energy groups by a given percentage (equivalent to an increase in the density of these materials) was predicted, and the prediction was then compared with the dose change as determined by a recalculation of the problem using ANISN with the perturbed cross sections. The change in dose with respect to change in the iron cross sections appears quite linear out to perturbations of the order of 5%, but non-linear effects are apparent in the 5% perturbations for sodium. Perturbations of the total collision cross section for only one important group in the sodium clearly indicates the non-linearity effect for this problem. This result may at least partially be explained by the importance of small angle scattering at high energies in the sodium which gives rise to a process approximating continuous slowing-down, thereby strongly coupling the fluxes in each group. In contrast, the iron one-group perturbation remains fairly linear, despite

Table 2. A Comparison of Predicted Changes in Dose Due to Cross-Section Perturbations Versus Calculated Results Obtained With the Perturbed Cross Sections

Sodium			Iron		
Cross-Section Perturbation in Collision (%)	Predicted Change in Tissue Dose (%)	Recalculated Change in Tissue Dose (%)	Cross-Section Perturbation in Collision (%)	Predicted Change in Tissue Dose (%)	Recalculated Change in Tissue Dose (%)
+ 0.1, all groups	- 1.797	- 1.712	+ 0.1, all groups	- 0.391	- 0.376
+ 0.5, all groups	- 8.99	- 8.26	+ 0.5, all groups	- 1.955	- 1.87
+ 1.0, all groups	- 17.97	- 15.84	+ 1.0, all groups	- 3.91	- 3.72
+ 5.0, all groups	- 89.85	- 57.45	+ 5.0, all groups	- 19.55	- 17.25
+ 1.0, group 25	- 1.53	- 1.42	+ 1.0, group 30	- 1.58	- 1.48
+ 10.0, group 25	- 15.3	- 10.1	+ 10.0, group 30	- 15.8	- 13.1
- 1.0, group 25	+ 1.53	+ 1.55	- 1.0, group 30	+ 1.58	+ 1.52
- 10.0, group 25	+ 15.3	+ 25.0	- 10.0, group 30	+ 15.8	+ 17.4

the fact that the group perturbed contains the 24.5 keV iron minimum. While this effect is not completely understood, it is noted that elastic collisions in iron result in less energy loss per collision than those in sodium. Perturbations which involve a decrease in the sodium total collision cross section were included to illustrate that the linear approximation tends to underpredict the effect of a cross-section decrease, but tends to overpredict the effect of a cross-section increase for this problem.

In addition to predictions based on linear perturbation theory, an attempt has been made to predict the effects of truncating by group the number of moments used in the Legendre expansion of the scattering kernel. In this case, δT_{Σ} in Equation 4 represents the moments of the scattering cross sections eliminated from the original P_3 calculation. The truncation by group was then adjusted to give approximately equal errors in each group with a total error of less than 0.1%. Other cases involving more radical truncations were also considered.

The predictions are compared with recalculated results in Table 3. In the first case, the number of Legendre moments was varied by group for both sodium and iron, and, as shown, the tissue dose obtained from an ANISN recalculation was within 0.1% of the original calculation. Although most transport codes are not currently equipped to handle a variation in the number of Legendre moments by group, it can easily be done, and the results here indicate that such a calculation might result in a significant reduction in running time with little loss in accuracy, especially for two-dimensional codes. The remaining cases show that for this problem, the tissue dose calculated when iron is run with a P_0 ex-

Table 3. PREDICTED VERSUS RECALCULATED VARIATION OF THE TISSUE DOSE WITH NUMBER OF LEGENDRE MOMENTS USED IN THE ANGULAR EXPANSION

Number of Moments		Predicted Change in Tissue Dose From Initial P_3 (%)	Recalculated Change in Tissue Dose From Initial P_3 (%)
Sodium Energy Groups	Iron Energy Groups		
P_3, 1-12	P_1, 1-10		
P_2, 13-26	P_2, 11-20	- 0.07	- 0.03
P_1, 27-32	P_1, 21-50		
P_0, 33-50			
P_3, 1-12			
P_2, 13-25			
P_1, 27-32	P_0, all groups	- 20.8	- 16.8
P_0, 33-50			
P_1, all groups	P_1, all groups	- 18.0	- 13.8
P_0, all groups	P_0, all groups	- 278.0	- 87.6
P_1, all groups	P_0, all groups	- 39.0	- 27.1

pansion and sodium is run with a P_1 expansion is within 30% of the original P_3 dose calculation. Using a P_0 expansion for sodium, however, causes a large change in the tissue dose. All the calculations used an S_{16} Gaussian Legendre quadrature so that these conclusions do not imply that diffusion theory is adequate for this system.

III. CONCLUSIONS

In conclusion, the results presented provide confirmation of the usefulness of a quantitative definition of sensitivity. The physical meaning implicit in the definition made it possible to determine directly the important reaction cross sections, in an energy-dependent fashion, for the problem studied. Furthermore, the predictive aspect of the definition is consistent with a perturbation theory approach and with the potential for evaluating the effects of cross-section uncertainties and the effects of approximate representation of basic cross-section data.

For the specific sodium-iron problem studied, the sensitivity analysis provided substantial confirmation of the role of total cross-section minima in deep penetration. The dominant effect of the 24.5 keV window in iron was demonstrated quantitatively, in a manner that was expected, but the substantial importance of the sodium minima in the 1 to 3 MeV range was also revealed. Predictions concerning the number of Legendre expansion terms needed to represent both the sodium and iron scattering kernels were quite enlightening in that a P_1 representation for both sodium and iron were concluded to be adequate for this problem. Corroboration of this conclusion with recalculations pointed out one of the stronger predictive applications possible with this kind of sensitivity technique.

Finally, we expect that future extensions of this method will reveal the real promise of the method as a tool for both analysis and prediction. Development plans include the coupling of the technique to extremely fine energy-dependent point cross-section calculational methods (using up to 1000 energy point grids) for analyzing energy-dependent reaction rates in great detail and also for use in an importance-weighted group-averaging scheme. In more practical application, the method should prove to be extremely helpful in designing and analyzing integral experiments which will be more relevant, in the sense of having similar sensitivity to cross sections, to real design problems. The predictive aspect of the method should also be able to provide quantitative estimates of design result uncertainties based on the inadequacies in any reaction cross-section set. These estimates, to be generally applied, however, will have to be the result of further development work on practical methods for calculating perturbed adjoints.

REFERENCES

1. G. E. Hansen and H. A. Sandmeier, "The Effect of Basic Neutron Reaction Cross Sections of Nitrogen (n,n'), (n,2n), (n,γ), (n,p), and (n,α) on High Energy Neutron Penetration in Air," LA-3810, Los Alamos Scientific Laboratory, 1967.

2. E. A. Straker, "Sensitivity of Neutron Transport in Oxygen to Various Cross-Section Sets," ORNL-TM-2252, Oak Ridge National Laboratory (1968).

3. W. E. Preeg, "Flux Sensitivity to Cross-Section Data for Iron and Oxygen," Doctoral Thesis, Columbia University (1970).

4. S. Hui, D. Spielberg, H. Steinberg, E. S. Troubetzkoy, and M. Kalos, "SAMCEP: An Application of Correlated Monte Carlo to the Simultaneous Solution of Multiple, Perturbed, Time-Dependent Neutron Transport Problems on Complex Three-Dimensional Geometry," BRL-CR-62, Ballistic Research Laboratories, Aberdeen Proving Ground (1972).

5. L. N. Usachev, "Perturbation Theory for the Breeding Ratio," J. Nucl. Energy A/B 18, 571 (1964).

6. P. C. E. Hemment et al., "The Multigroup Neutron Transport Perturbation Program DUNDEE," AWRE Report 040/66 (1966).

7. D. L. Prezbindowski and H. A. Sandmeier, "The Effects of Cross-Section Inaccuracies on Integral Data," Trans. Am. Nucl. Soc. 11, 193 (1968).

8. W. W. Engle, Jr., "A User's Manual for ANISN, A One-Dimensional Discrete Ordinates Transport Code with Anisotropic Scattering," K-1693, Computing Technology Center, Union Carbide Corporation (1967).

9. W. S. Snyder and C. Neufeld, Radiation Research 6(1), 67 (1957).

10. F. R. Mynatt, F. J. Muckenthaler, and P. N. Stevens, "Development of Two-Dimensional Discrete Ordinates Transport Code with Anisotropic Scattering," CTC-INF-952, Computing Technology Center, Union Carbide Corporation (1969).

11. Private communication, J. A. Harvey (1972).

1-3. L. S. Abbott
4. R. G. Alsmiller, Jr.
5. J. Barish
6-15. D. E. Bartine
16. A. A. Brooks
17. A. R. Buhl
18. H. P. Carter
19. K. C. Chandler
20. R. L. Childs
21-22. C. E. Clifford
23. S. N. Cramer
24. N. F. Cross
25. M. B. Emmett
26. W. W. Engle, Jr.
27. G. F. Flanagan
28. W. E. Ford
29. R. M. Freestone, Jr.
30. N. M. Greene
31. M. L. Gritzner
32. W. O. Harms
33. O. W. Hermann
34. R. J. Hinton
35. T. J. Hoffman
36. L. B. Holland
37. W. H. Jordan
38. J. R. Knight
39. J. Lewin
40. T. A. Love
41. J. L. Lucius
42. R. E. Maerker
43. F. C. Maienschein
44. P. G. McCarty
45. B. J. McGregor
46. G. L. Morgan
47. G. W. Morrison
48. F. J. Muckenthaler
49-53. F. R. Mynatt
54-58. E. M. Oblow
59. J. V. Pace
60. R. W. Peelle
61. S. K. Penny
62. F. G. Perey
63. A. M. Perry
64. L. M. Petrie
65. V. Rado
66. W. A. Rhoades
67. H. E. Seagren
68. A. H. Snell
69. P. N. Stevens
70. J. G. Sullivan
71. D. Sundberg
72. D. B. Trauger
73. D. K. Trubey
74. J. E. White
75. G. E. Whitesides
76. L. R. Williams
77. H. A. Wright
78. R. Q. Wright
79. H. Feshbach (consultant)
80. H. Goldstein (consultant)
81. C. R. Mehl (consultant)
82. H. T. Motz
83-84. Central Research Library
ORNL Y-12 Technical Library
85. Document Reference Section
86-90. Laboratory Records
91. Laboratory Records ORNL RC
92-101. Mathematics Division Library
102. ORNL Patent Office

EXTERNAL DISTRIBUTION

103. R. Avery, Director, Applied Physics Division, Argonne National Laboratory, 9700 S. Cass Ave., Argonne, Ill. 60439

104. R. Balent, Vice President, Power Systems Programs, Atomics International, P. O. Box 309, Canoga Park, California 91304

105. E. T. Boulette, Radiation and Shield Analysis, WADCO, P. O. Box 1970, Richland, Washington 99352

106. W. L. Bunch, Radiation and Shield Analysis, WADCO, P. O. Box 1970, Richland, Washington 99352

107. D. K. Butler, Argonne National Laboratory, 9700 S. Cass Avenue, Argonne, Ill. 60439

108. E. G. Case, Director, Division of Reactor Standards, U. S. Atomic Energy Commission, Washington, D. C. 20545

109. D. F. Cope, USAEC Site Rep., ORNL

110. J. W. Crawford, Division of Reactor Development and Technology, U. S. Atomic Energy Commission, Washington, D. C. 20545

111. J. B. Dee, Head, GCFBR Reactor Engineering, Gulf General Atomic, P. O. Box 608, San Diego, California 92112

112. R. K. Disney, Westinghouse Electric Corp., Advanced Reactor Division, P. O. Box 158, Waltz Mill Site, Madison, Pa. 15663

113. M. W. Dyos, Westinghouse Electric Corp., Waltz Mill Site, P. O. Box 158, Madison, Pa. 15663

114. R. Ehrlich, Manager, Advanced Development Activity, Knolls Atomic Power Laboratory, General Electric, P. O. Box 1072, Schenectady, N. Y. 12301

115. L. F. Fidrych, Manager, Design Engineering, Breeder Reactor Development Operation, General Electric, 310 DeGuigne Drive, Sunnyvale, California 94086

116. P. F. Fox, Westinghouse Electric Corp., Advanced Reactor Division, Waltz Mill Site, P. O. Box 158, Madison, Pa. 15663

117. W. E. Fry, U. S. Atomic Energy Commission, P. O. Box 550, Richland, Washington 99352

118. J. G. Gallgher, Deputy Manager, Engineering, WADCO, P. O. Box 1970, Richland, Washington 99352

119. P. F. Gast, Argonne National Laboratory, 9700 S. Cass Ave., Argonne, Ill. 60439

120. S. A. W. Gerstl, Argonne National Laboratory, 9700 S. Cass Ave., Argonne, Ill. 60439

121. P. Greebler, General Electric Co., Breeder Reactor Development Operation, 310 DeGuigne Dr., Sunnyvale, California 94086

122. J. P. Hamric, Division of Reactor Development and Technology, U. S. Atomic Energy Commission, Washington, D. C. 20545

123. W. H. Hannum, Division of Reactor Development and Technology U. S. Atomic Energy Commission, Washington, D. C. 20545

124. P. B. Hemmig, Division of Reactor Development and Technology, U. S. Atomic Energy Commission, Washington, D. C. 20545

125. P. L. Havenstein, Chief, Instrumentation and Control Branch, U. S. Atomic Energy Commission, Washington, D. C. 20545

126. P. L. Hofmann, Manager, Systems Analysis, WADCO, P. O. Box 1970, Richland, Washington 99352

127. T. Iltis, RDT Site Office, U. S. Atomic Energy Commission, P. O. Box 154, Madison, Pa. 15663

128. W. M. Jacobi, Westinghouse Electric Corp., ARD, P. O. Box 158, Waltz Mill Site, Madison, Pa. 15663

129. Dr. V. A. Kamath, Scientific Advisor, Attn: P. K. Patwardhan, Bhabha Atomic Research Centre, Trombay, Bombay, India

130. E. E. Kintner, Division of Reactor Development and Technology, U. S. Atomic Energy Commission, Washington, D. C. 20545

131. K. O. Laughon, USAEC Site Representative, ORNL

132. J. W. Lewellen, Division of Reactor Development and Technology, U. S. Atomic Energy Commission, Washington, D. C. 20545

133. W. B. Loewenstein, Argonne National Laboratory, 9700 S. Cass Ave., Argonne, Ill. 60440

134. C. P. McCallum, Division of Space Nuclear Systems, U. S. Atomic Energy Commission, Washington, D. C. 20545

135. P. A. Morris, Director, Division of Reactor Licensing, U. S. Atomic Energy Commission, Washington, D. C. 20545

136. P. M. Murphy, Manager, Advanced Engineering, General Electric, Sunnyvale, California 94086

137. T. A. Nemzek, U. S. Atomic Energy Commission, P. O. Box 550, Richland, Washington 99352

138. R. J. Neuhold, Division of Reactor Development and Technology, U. S. Atomic Energy Commission, Washington, D. C. 20545

139. Prof. P. F. Pasqua, Department of Nuclear Engineering, University of Tennessee, Knoxville, Tennessee

140. N. A. Petrick, Manager, LMFBR Project, Advanced Reactor Division, Westinghouse Electric Corp., Waltz Mill Site, P. O. Box 158, Madison, Pa. 15663

141. T. A. Pitterle, Westinghouse Electric Corp., Advanced Reactor Division, Waltz Mill Site, P. O. Box 158, Madison, Pa. 15663

142. J. L. Rathbun, Westinghouse Electric Corp., ARD, Waltz Mill Site, P. O. Box 158, Madison, Pa. 15663

143. D. R. Riley, Chief, Core Design Branch, Division of Reactor Development and Technology, U. S. Atomic Energy Commission, Washington, D. C. 20545

144. T. Rockwell, MPR Associates, Inc., 1140 Connecticut Ave. NW, Washington, D. C. 20036

145. J. N. Rogers, Division 8321, Sandia Laboratories, P. O. Box 969, Livermore, California 94550

146. Dr. Milton E. Rose, Mathematics and Computer Branch, Division of Research, U. S. Atomic Energy Commission, Washington, D. C. 20545

147. M. A. Rosen, Division of Reactor Development and Technology, U. S. Atomic Energy Commission, Washington, D. C. 20545

148. W. J. Rowan, Westinghouse Electric Corp., Advanced Reactor Division, Waltz Mill Site, P. O. Box 158, Madison, Pa. 15663

149. M. Shaw, Director, Division of Reactor Development and Technology, U. S. Atomic Energy Commission, Washington, D. C. 20545

150. E. E. Sinclair, Division of Reactor Development and Technology, U. S. Atomic Energy Commission, Washington, D. C. 20545

151. B. J. Snyder, Division of Reactor Development and Technology, U. S. Atomic Energy Commission, Washington, D. C. 20545

152. E. R. Specht, Atomics International, P. O. Box 309, Canoga Park, California 91304

153. W. P. Staker, Manager, Fast Breeder Development, Combustion Engineering, Windsor, Conn. 06095

154. D. G. Stenstrom, Argonne National Laboratory, 9700 S. Cass Ave., Argonne, Ill. 60440

155. A. N. Tardiff, Division of Reactor Development and Technology, U. S. Atomic Energy Commission, Washington, D. C. 20545

156. J. J. Taylor, General Manager, Westinghouse Electric Corp., ARD, Waltz Mill Site, P. O. Box 158, Madison, Pa. 15663

157. M. L. Weiss, General Electric Co., Breeder Reactor Development Operation, 310 DeGuigne Dr., Sunnyvale, California 94086

158. Technical Information Center (TIC)

159-160. Research and Technical Support Division

161-297. Given DNA Radiation Transport Distribution

298-433. Laboratory Records for FREF Distribution